USING INTEGRATED COLOR AND TEXTURE FEATURES FOR AUTOMATIC HAIR DETECTION

Uri Lipowezky[1], Omri Mamo[2], and Avihai Cohen[2]

[1]Samsung Semiconductor,
[2]Jerusalem College of Technology – Machon Lev, Department of Electronics

ABSTRACT

Hair is one of the most challenging facial features, playing important role in human appearance. This paper introduces novel approach to human hair extraction, based on integration of texture, shape and color features. This approach allows robust hair detection in complex background under various illumination and hairstyles. This study deals with color images and hair detection aims hair re-colorization to simulate different hair colors. The process starting with typical facial features extraction such as open skin, eyes and mouth and finishing with fuzzy hair mask. Fuzzy hair representation allows overcoming hair appearance problems around hair roots and close to outer line of hairstyle. Fuzzy hair mask building involves binary hair mask detection, background detection and matting procedure. Experiments caring in cosmetic store environment for 354 images show 75% of correct detection for complex background and illumination and 85% for homogeneous background and illumination.

Index Terms—Face recognition, feature extraction, fuzzy logic, color, clustering methods

1. INTRODUCTION

Human hair is one of the most challenging features in facial analysis. It is very complex visual pattern consisting of different types of color textures. It has been suggested [2] that hair plays important role in face recognition, human animation and non-photorealistic rendering. This study is dealing with hair detection in order to simulate hair color on user hair without changing hairstyle. This simulation shows up very attractive for virtual cosmetic product simulators such as [15], [16]. There are three reasons making this application especially challenging.

- First, human can drastically manipulate with their hair such as a variety of hairstyles, colors and xenoliths inside of hair such as gums, bandanas, cookies etc. This yields drastic variability of hair appearance.

- Second, complex background of the user's photo taken with stand alone kiosk in cosmetic store e.g., [12] produces additional difficulties to separate hair from background. The situation becomes especially complicated when another user's hair appearances on the background.

- Third, illumination in user's photo is not as optimal as in model's photo reproduced on hair color boxes. This leads to inevitable change of hair color and texture at different location: i.e., side swatch of hair might quite differs from the swatch near the roots.

There is very little prior work on hair detection. In the most pioneer study [7] it was shown possibility of hair extraction by using textural features: gray level co-occurrence matrix, gray level difference vector, gray level run length matrix and neighborhood gray level dependence matrix. Study [13] proposes hair detection using Farnsworth's non-linear transform of colors. Hair color similarity map (HCSM) is calculated for every image pixel. The HCSM is combined with skin color similarity map for fuzzy pattern matching between face photos. They reported about 91% correct detected dark hair on homogeneous background; however, no treatment for blond hair is given. The most fundamental study on hair detection [14] exploits color difference between RGB of face skin and hair. They introduced hair region of interest (RoI), consisting of forehead rectangle and two side rectangles and iterative process of hair region growing, starting with hair seed color. Authors report about 71% of successful hair detection on 524 face data set.

In this paper method Yacoob and Davis [14] is extended by using as color as textural features with respect to face skin detection. Hair region is modeled as fuzzy mask $H(x,y) \in [0,1]$, where $H(x,y) = 0$ corresponds to non-hair pixel (x,y) and $H(x,y) = 1$ corresponds to definitely hair pixel. Study [14] exploits chromaticity and intensity difference between open skin and hair in order to define seed region, inner and outer hair line. In this paper chromaticity and intensity difference is integrated with texture features. The using of texture features allows extracting hair from complex background and diminishes local changes of hair color inevitable for colorized color and changes in local hair illumination. Hair mask (see fig. 1f) is obtained as result of Alpha-Matting procedure [8]: $I = FH + B(1-H)$, where I is original color image (fig 1a), F is foreground (hair) image and B is background (non

hair) image. Matting process is applied to tri-map (fig 1e), which consists of definitely hair, definitely background and unknown regions. Hair detection starts with extracting of facial feature such as open skin, mouth and eyes (fig. 1b). This process is based on P. Viola and M. Jones face detector [11] combined with fuzzy C-mean clustering. Hair detection process is subdivided into seed hair region detection (fig 1c) and hair seed region growing (fig 1d). Hair seed detection is based on synergy mean shift segmentation technique (EDISON) [3]. For each segment a number textural, color, shape and topological features are calculated. Gentle boosting technique [4] is applied to accept or decline the checked segment. The binary hair detection is obtained as result of clustering procedure. Experiments with real images and are accomplished the study.

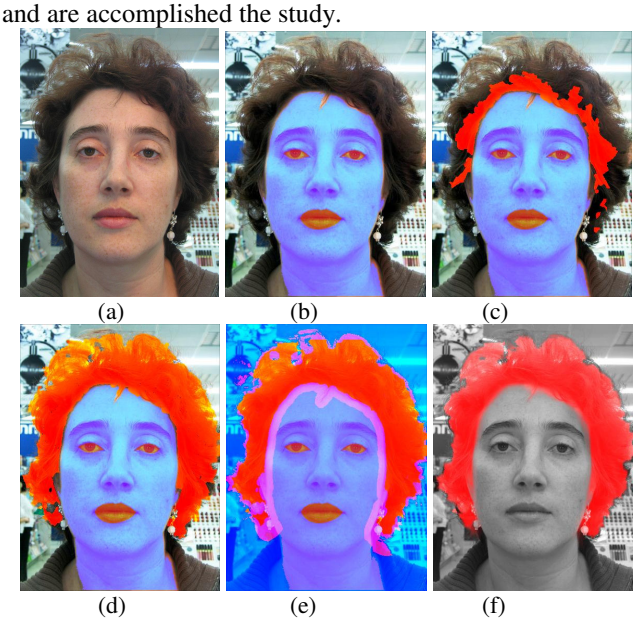

(a) (b) (c)

(d) (e) (f)

Fig. 1. Hair detection process: (a) original photo, (b) extracted facial features, (c) seed hair areas, (d) preliminary hair detection, (e) tri-map, (f) final hair mask after the matting.

2. HAIR SEED AREA DETECTION

The hair detection process starts with facial features extraction such as open skin, mouth and eyes (see fig. 1b). This process is left beyond of the scope of our study and briefly is described in [10]. Let us suppose that these features are known with reasonable accuracy before hair detection is starting (see fig 1b). As well let us assume that person that hair to be detected has hair over forehead. Under this assumption seed hair area as defined as shown in fig. 2a. The image is rotated with respect to eyes location and scaled to 1024x768 pixels as well for dark or low-contrast images histogram equalization is applied. Seed hair RoI is defined as follows: upper margin is $U_y = \min\left(E_y^L, E_y^R\right) - 1.6h$, where h is the length of mouth central point projection to inter-eyes line $\left(E^L, E^R\right)$, where E^L and E^R are left and right eye center. Down RoI margin is defined as $D_y = \min\left(E_y^L, E_y^R\right) - 0.1h$, left margin is $L_x = C_x^L - 0.5B$, and right margin is $R_x = C_x^R + 0.5B$, where C^L and C^R r are external left and right eyes' cantus and $B = \left\|E^L, E^E\right\|$ is inter-eyes distance. Regardless facial feature, original color image is over segmented using EDISON algorithm [3] with the following parameters. Mean shift spatial bandwidth $h_s = 7$ pixels, color bandwidth $h_r = 10$ bins and minimal region size $M = 100$ pixels. Along with mean shift clustering synergetic segmentation [3] is applied for gradient window $n = 5$ pixels, mixed parameter $a_{ij} = 0.5$ and threshold $t_e = 0.4$. An example of over-segmented hair image is given in fig. 2b. Regarding every segment from RoI it should be decided does this segment belongs to hair or not.

(a) (b)

Fig. 2. RoI for hair seed detection (a) and over-segmented resulted from EDISON algorithm (b).

Besides EDISON segmentation 3 color features (CIE La^*b^*), Canny magnitude [1] and 4 textural features are calculated per pixel (micro-features). The textural features are based on two-level Haar wavelet decomposition. For sub-bands LH, HL and HH standard deviation in 3x3 square window is calculated and features $\sigma(LH)$ and $\sigma(HL)$, where $\sigma(.)$ denotes the standard deviation are combined into new feature $W = \alpha\sigma(LH) + \beta\sigma(HL)$ in order to provide robustness to change of hair swatch direction. Factors α and β are derived from results [9] as $\alpha = \sin\varphi$ and $\beta = \cos\varphi$, where $\varphi = 0.5 \arctan\left|2\rho\sigma_{LH}\sigma_{HL} / \left(\sigma_{LH}^2 + \sigma_{HL}^2\right)\right|$, where ρ, σ_{HL} and σ_{HL} are correlation ratio and the standard deviations of $\sigma(LH)$ and $\sigma(HL)$ features inside the hair seed RoI area. Some of micro-features are displayed in fig. 3. Using these micro-features the following macro-features (per segment) are calculated. There are 5 topological features, 5 morphological and 3 textural features.

(a) (b) (c)

Fig. 3. Micro-features for hair seed detection: Canny magnitude (a), W_1 for the first level sub-bands (b) and W_2 for the second level (c).

The principle idea behind these features is to detect segments distinct from open skin on one hand and having natural texture on the other hand to be different from the background. It is assumed that there is no another person's hair in the seed hair RoI. The following topological features are used. Percent of segment pixels detected as facial features t_F .If $t_F > 90$ it is assumed that segment belongs to the face. $d_{\min} = \min(D/B)$ and $d_{\max} = \max(D/B)$, where D is the distance from segment pixel to open skin and B is inter-eyes distance. $\bar{\theta} = E[|\theta|]$ and $\Delta\theta = \max\theta - \min\theta$, where θ is the pixel angular coordinate with regard to the middle of down RoI bound defined in [14] as glabella (see fig. 2a). The segment shape is described using morphological features: $t_s = N_{seg}/N_{sk}$, where N_{seg} is the number of pixel in the segment and N_{sk} is the number of pixels in the open skin. Shape factor $K_f = 400\pi S/P^2$, where S is the segment area and P is the segment perimeter. Convex hull factor $ch = (S_{ch} - S)/S$, where S_{ch} is convex hull segment area and hole factor $hl = (S_f - S)/S$, where S_f is filled area. Statistical difference between the open skin and hair is emphasized using textural features such as Wilks ratio $W = \sqrt{|\Sigma_{seg}|/|\Sigma_{sk}|}$, where Σ_{seg} and Σ_{sk} are micro-features covariance for the segment and the open skin. Bhattacharyya distance for Gaussian distribution and equal hair – non-hair a priory probability:

$$\mu_{1/2} = \frac{1}{8}(\Delta M)^T \Sigma_0^{-1}(\Delta M) + \frac{1}{2}\ln\left(|\Sigma_0|/\sqrt{|\Sigma_{sk}||\Sigma_{seg}|}\right),$$

where $\Sigma_0 = (\Sigma_{sk} + \Sigma_{seg})/2$, $\Delta M = M_{seg} - M_{sk}$, M_{seg} and M_{sk} are micro-features averages. Hotelling t-ratio [5] for Gaussian distribution:

$$t = \sqrt{(\Delta M)\tilde{\Sigma}^{-1}(\Delta M)^T \left(\frac{N_{sk} + N_{seg} - d - 1}{N_{sk} + N_{seg} - 2}\right)\left(\frac{N_{sk}N_{seg}}{N_{sk} + N_{seg}}\right)},$$

where d is the number of micro-features. These macro-features are used as input for gentle boosting classifier [4]. Eventually 3256 manually detected segments: 2200 hair and 1056 non-hair were used for 3-cascade boosting training.

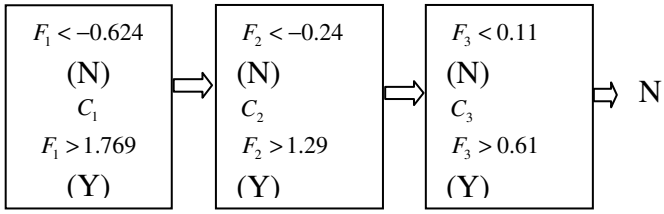

Fig. 4. Three cascade gentle boosting detector for seed hair.

For each cascade output function is calculated as: $F = \sum_{i=1}^{M} a_i(\varphi_i > t_i) + b_i$, where M is the number of week classifiers or stumps: actually there are 175-250 stump for different cascades, φ_i is the value of macro-feature for stump i, t_i is its threshold, a_i and b_i are stamp parameters. Value F is tested with two thresholds: $F > F_{\max}$, where $F_{\max} > 0$ for definitely hair, $F < F_{\min}$, where $F_{\min} < 0$ for definitely non-hair, otherwise segment is tested with the next cascade (see fig. 4). If the decision is not taken with the last cascade non-hair decision is accepted by default. The values of $F_{\max}$ and $F_{\min}$ along with cascade boosting flowchart are displayed in fig. 4. Some results of hair seed detection are shown in fig 5.

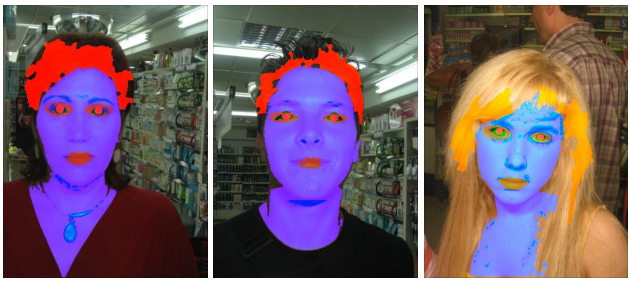

Fig. 5. Examples of hair seed detection on complex background.

3. HAIR REGION GROWING

Set of 45 features is examined and some of features are selected for detection of the whole hair region. The subset of 14 features is based on color components from RGB, YC_bC_r and La*b* color spaces. Besides, 6 additional features, based on color RGB and YC_bC_r component values deviation from the seed color sampling are included. These seed dependent features include calculation the Euclidian distance $\|\bar{c} - \bar{c}_s\|$ from the average seed color $\bar{c}_s = (c_{s1}, c_{s2}, c_{s3})$, cylindrical distance $\|\bar{c} - \alpha\bar{c}_s\|$, where $\alpha = \sum_{i=1}^{3} c_i c_{si} / \|\bar{c}_s\|^2$ minimizes the distance from plane $\beta c_1 + \gamma c_2 + \delta c_3 + \varepsilon = 0$, which fits the seed samples color with respect to MLS error. The set of 7 additional features, based on the Sobel filter reply, Haar wavelet decomposition and orientation filter in frequency domain, are used to define the magnitude of the image gradient. A number of features are used to emphasize strong image

change. There are the standard deviation filters before and after Laplacian filter, range filter and the difference between the original grayscale image and reply of iterative open-closing morphological filter. The group high-order statistics includes kurtosis, skewness and entropy. The last group of features including 6 features studied in [5] and 4 Gabor-based features: sums of reply in different orientations and scales. The latter group provides separation between textures. The final set of the selected features depends on the hair chromaticity and intensity. The decision regarding the hair color is made in HSV color space, whereas the color can be "blond", "brown", "red", "white" and "black", and the intensity can be "low", "medium" and "high". Besides, the set of features is divided into 4 subsets: color based features, seed-based features, gradient features, and textural features. Each subset defines a vector of feature values $\overline{f} = (f_1, f_2, ..., f_n)^T$ that is sent to k-mean clustering procedure. Following study [4] the weight of each feature is $w_l = 0.5 \ln\left[(1-e_l)/e_l\right]$, where e_l is experimentally estimated classification error between hair and background for feature f_l. A pixel is denoted by label A if $P(B)/P(A) > \gamma$ for every label $B \neq A$ and $P(A) \geq P_{\min}$. Parameters γ and $P_{\max}$ are chosen to allow the region be labeled as "hair" if it contains at least 15% of seed pixels. The procedure is done for $k = 3,...,7$ clusters and the most common decision is selected: whether a pixel is hair or not. Using these 4 hair maps from each subset, the final map is generated as a logic "and" between the maps. The process is accomplished with post-processing, including morphological cleanup. An example of hair region growing is shown in fig. 6.

(a) (b) (c)

Fig.6. Hair region growing: hair seed (a), clustering (b) binary hair mask (c).

4. HAIR TRIMAP DETECTION

Having detected the binary hair area, definitely background region should be detected as well in order to apply matting procedure [8]. Hair root areas are detected by diminishing by $B/20$, where B is the inter-eyes distance as for hair as for open skin clusters along skin-hair boundary (see fig. 1e). Definitely background pixels could be detected as follows. Let us suppose that hair micro-feature distribution is Gaussian. Because wavelet-based features express the standard deviations, having χ^2-based distribution logarithmic transform could be applied. Therefore, new micro-features are calculated as $\ln(\sigma(.))$ have near-Gaussian distribution. If a is Mahalonobis distance between pixel's micro-features vector X and hair prototype (M, Σ), i.e. $a = (X-M)\Sigma^{-1}(X-M)^T$ than probability that pixels, having distances $\rho \leq a$ belongs to hair is

$$\mathrm{P}(X \in H \mid \rho \leq a) = \int_0^a e^{-\rho^2/2} \rho^{n-1} d\rho \left(\prod_{k=1}^{n-2} \int_0^{\pi} \sin^k \varphi_k d\varphi_k \right) \int_0^{2\pi} d\varphi_{n-1} \qquad (1)$$

Having taken right hand integrals equation (1) compressed to $G(a) = \frac{2\pi^{n/2}}{\Gamma(n/2)} \int_0^a \rho^{n-1} e^{-\rho^2/2}$, where n is the number of micro-features and Γ denotes gamma-function. Eventually integral (1) is expressed as

$$G(a) = \frac{2^{(n+10)/4} e^{-a^2/4}}{\Gamma\left(\frac{n}{2}\right)} \left[\frac{a^n M\left(\frac{n}{4}, \frac{n+2}{4}, \frac{a^2}{2}\right)}{n(n+2)} + \frac{a^{n-2} M\left(\frac{n+4}{4}, \frac{n+2}{4}, \frac{a^2}{2}\right)}{n} \right],$$

where M is Whittaker's M-function. Inverting $G(a) = p$ yields maximal Mahalanobis distance in quest. Fig. 7 shows relationship a with respect to n and p.

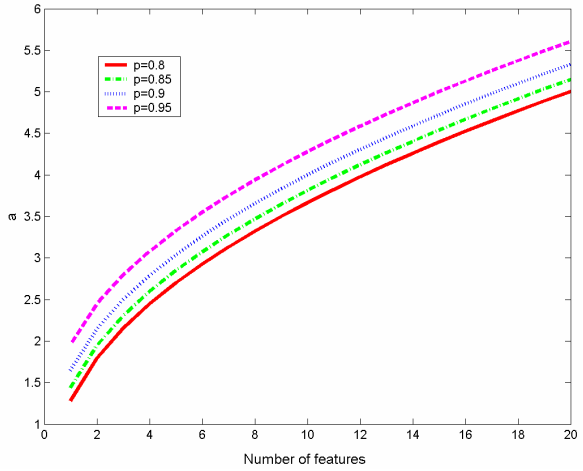

Fig. 7 Relationship a with respect to n and p.

Fig. 8. Examples of tri-map detection.

Pixels having Mahalanobis distance $a > G^{-1}(p)$ where $p = 0.95$ denote as background pixels. Examples of tri-map detection are shown in fig. 8.

5. CONCLUSION

The proposed method of automatic hair detection was tested on database of 354 images: 147 Images with homogeneous background and 207 images with complex background of cosmetic store. Experiments show overall accuracy for visual perception of 85% of correct (accepted) hair detection for homogeneous background and 75% for complex background. Examples of successful and unsuccessful hair detection are displayed in fig. 9.

Fig. 9. Examples of successful (a-c) and unsuccessful (d-f) hair detection.

The main impact of the proposed study seems to be principle possibility of full automatic hair detection. Obtained fuzzy hair mask opens wide perspective for high-quality photorealistic hair re-colorization and other potential applications. However, there are two main directions for future work. The first is the performance improvement because full process of hair detection takes up to 5 minutes processing time for conventional PC. The second one is accuracy improvement while hair mask manually correction is not trivial task for cosmetic store user [12], [15], [16]. The most important task in this direction is the selection of good textural features for separating hair texture from the background.

6. REFERENCES

[1] J. Canny, "A Computational Approach to Edge Detection," *IEEE Trans. on Pattern Analysis and Machine Intelligence*, vol. 8, no. 6, pp. 679-697, November 1986.

[2] H. Chen, and S-C. Zhu, "A Generative Sketch Model for Human Hair Analysis and Synthesis," *IEEE Trans. on Pattern Analysis and Machine Intelligence*, vol. 28, no. 7, pp. 1025-1040, 2006.

[3] C. Christoudias, B. Georgescu, and P. Meer, "Synergism in Low Level Vision," *Proc. 16th Int'l Conf. Pattern Recognition*, vol. 4, pp. 150-155, August 2002.

[4] J. Friedman, T. Hastie, and R. Tibshirani, "Additive Logistic Regression: A Statisical View of Boosting", *The Annals of Statistics*, vol. 28, no. 2, pp. 337-407, 2000.

[5] M. Haley, and B. S. Manjunath "Rotation-Invariant Texture Classification Using a Complete Space-Frequency Model" *IEEE Trans. on Image Processing* vol. 8 no. 2, pp. 255-269, 1999.

[6] H. Hotelling, "The generalization of student's ratio," *Ann. Mathematical Stat.*, vol. 2, pp. 360–378, 1931.

[7] Jia, X., *Extending the Feature Set for Automatic Face Recognition*. PhD dissertation., Univ. of Southampton. 1993.

[8] A. Levin, D. Lischinski, and Y. Weiss, "A Closed-Form Solution to Natural Image Matting," *IEEE Trans. on Pattern Analysis and Machine Intelligence*, vol. 30, no. 2, pp. 228-242, 2008.

[9] U. Lipowezky, Y. Furth, and E. Luson,"Unsupervised Classifying Land Development in High Resolution Multi - Spectral Satellite Photos and Application for Facial Features Extraction," *Proc. 23-th Convention IEEE in Israel*, pp. 426-431, 2004.

[10] U. Lipowezky, and S. Cahen, "Automatic Freckles Detection and Retouching," *Proc. 25-th Convention IEEE in Israel*, 2008.

[11] P. Viola, and M. Jones, "Robust Real-Time Face Detection," Int'l *J. Computer Vision*, vol. 57, pp. 1473-1505, 2004.

[12] J. M. Wilmott, D. T. Aust, and T. K. Crawford, "Method for producing customized cosmetic and pharmaceutical formulations on demand*", United States Patent 6782307*, 24 August 2004.

[13] H. Wu, Q. Chen, and M. Yachida, "Face Detection from Color Images Using a Fuzzy Pattern Matching Method," *IEEE Trans. on Pattern Analysis and Machine Intelligence*, vol. 21, no. 6, pp. 557-563, 1999.

[14] Y. Yacoob, and L. S. Davis, "Detection and Analysis of Hair," *IEEE Trans. on Pattern Analysis and Machine Intelligence*, vol. 28, no. 7, pp. 1164-1169, 2006.

[15] http://www.ezface.com. *EZface Virtual Mirror*. EZface Inc., 2008.

[16] http://www.taaz.com. Taaz.com/Photometria Inc., May, 2008.